

## Theoretical Study of the Radiological Properties of NIPAM Polymer Dosimetry Gel

Swait S. Mohammed<sup>1</sup>, Israa F. Al-Sharuee<sup>1,\*</sup>, Akram Mohammed Ali<sup>2</sup>

1. Department of Physics, College of Science, Mustansiriyah University, Baghdad, IRAQ

2. Department of Physics, College of Science, University of Anbar, IRAQ

\*Corresponding author E-mail: [i81f54@uomustansiriyah.edu.iq](mailto:i81f54@uomustansiriyah.edu.iq)

<https://doi.org/10.29072/basjs.20240217>

### ARTICLE INFO

### ABSTRACT

#### **Keywords**

NIPAM gel, dosimetry gel, Zeff, gel/water-equivalent, cross-section

The NIPAM offers significant potential for use as a three-dimensional dosimeter in advanced radiation activities. To investigate and delineate its radiological properties, we employed various methodologies. Photon interaction cross-sections, mass energy absorption coefficients, effective atomic numbers, mean values of Zeff, and gel/water equivalence. Due to significant dependence on atomic number, photoelectric absorption cross sections exceed those of water for energies up to 10 MeV. The cross sections of Compton scattering and pair formation for NIPAM gel are differentiated from those of water. Photoelectric absorption is the primary mechanism of energy absorption in this range, resulting in NIPAM's mass-energy absorption coefficient being significantly higher than that of water. The principal findings were juxtaposed with those of osseous and soft tissue materials. The gel's Zeff has been found to correlate with water as effectively as with any other material, including bone and tissue. Dosimetry can be conducted utilizing NIPAM gel, which is considered water equivalent for both keV and MeV, as demonstrated by our results. These data suggest that NIPAM gel exhibits greater water equivalency compared to bone and tissue.

Received 9 Dec 2024; Received in revised form 23 Dec 2024; Accepted 27 Dec 2024, Published 31 Dec 2024



## 1. Introduction

The nuclear properties study of has attracted wide attention to understand the nuclear structure from many researchers and photon reaction scattering cross-section is studied with incident energy region [1]. In medical physics, dosimeters are very important in measuring radiation dose, although there are different types of dosimeters including 1D, 2D, and more recently 3D, which is an excellent gel dosimeter[2] because it has many advantages including tissue equivalents, no energy dependence, lower dose rate dependence and also works like reagents, which means no need for an energy perturbation correction factor[3]. The gel meter is divided into two parts: a Fricke gel (inorganic) and a polymer gel (organic). Polymeric gels are fabricated by gelatin, water, and building blocks called monomers such as acrylamide [4, 5], N-isopropyl acrylamide (NIPAM) [6, 7], acrylic acid [8], and n-vinylpyrrolidone [9, 10]. When radioactive sources are used, these monomers will be converted into a polymer called a polymer gel dosimeter. The converted monomers are used to measure the absorbed dose using several different techniques including magnetic resonance imaging (MRI), optical computed tomography (CT), X-ray computed tomography (XCT), and ultraviolet-visible spectrophotometry (UV-vis) [11-14]. From here, one can say that any material used in dosimetry must know its radiological properties, such as the effective atomic number based on the effective attenuation coefficient and the mass energy absorption coefficient. In this work, we will study and evaluate these radiological properties for one of the labeled polymers used in dosimetry with a synthetic formula ( $C_6H_{11}NO$ ) and a density of ( $1.13 \text{ g/cm}^{-3}$ ). The results will be compared with the other materials as bone and tissue.

## 2. Experimental

### 2.1 Radiological properties

Several considerations must be taken into account when choosing the gel formulation used in gel dosimeters. The first of these considerations is the extent to which the properties of the gel used match those of water, so it is necessary to make the necessary comparison of some parameters such as density, attenuation, stopping power, and effective atomic number [15]. Mosely was the first to determine the atomic number and how it is fundamentally related to the rest of the various properties of the element. In photon absorption studies [16, 17], the dependence of these reactions on the atomic number of the material was proven, which made the concept of the effective atomic



number, whether the water is a mixture or a compound, clear since this factor represents the attenuation property of the heterogeneous medium, which makes it helpful when making comparisons between gels and their equivalent water/textile ratio . There are several studies in which the  $Z_{\text{eff}}$  of water was calculated with its equivalent gel when used in (radiotherapy dosimetry) as in sources [4, 5]. Mayneor's calculations are mainly based on measurements of low energy attenuation Also when comparing radiologic properties,  $Z_{\text{eff}}$  is calculated to be taken into account within a certain energy range, and reliance on energy data is now very important when studying biological materials and other materials for the importance of dosimetry [18, 19]. In this study, the effective atomic number  $Z_{\text{eff}}$  of NIPAM gel will be calculated as a function of energy whose value will be from 10 keV to 10MeV. For comparison,  $Z_{\text{eff}}$  will be calculated for water, soft tissue, and bone as there will be a difference between the curves over the energy range used and cannot rely on a single value for  $Z_{\text{eff}}$  and this single value will be suitable for some applications, that require calculating or averaging the value according to the spectrum of the source used .

## 2.2 Theoretical Method Used in Calculations

When working on gel dosimetry, there were several methods used to determine  $Z_{\text{eff}}$ , including the method of Maynard [20], who gave the electronic fraction of the element  $i$ th in terms of  $f_i$  where  $\sum f_i=1$  within the equation used by [21]:

$$Z_{\text{eff}} = \sqrt[m]{\sum_{i=1}^n f_i Z_i^m} \quad (1)$$

Also, the work of Spies [22] on the mass absorption coefficient of energy in tissues using the expression used by Waters [23]for the photoelectric absorption coefficient, which is the linearity of the expression used by Mayneayd in the effective atomic number, all that means that the different reaction processes depend on the exponent  $m$  and therefore the calculation of  $Z_{\text{eff}}$  will give different calculations The effect of different reaction processes affects the total cross-section of the photon interaction with changing energy, and this is explained by Hine [24], where  $Z_{\text{eff}}$  must be different for each reaction, where  $m=3.1$  was used. for the photoelectric phenomenon and pair production, respectively, between them[25] . Weber and Berge proposed  $m=3.4, 1.7$ , with  $Z_{\text{eff}}$ . Many studies then appeared that used variable values of  $m$  to calculate  $Z_{\text{eff}}$  and whenever the energy limits do not include the large energy range, it must comparisons of radiative properties within this large energy range, and all types of interactions must be made



### 2.3 $Z_{\text{eff}}$ calculations

Since the transport of photons within a material is highly correlated with the energy and atomic number of the material [26] with the mass attenuation coefficient, this work will use the attenuation coefficient data that will be calculated knowing that the energy range of the incident photon will be from 10 keV to 10 MeV. The cross sections of NIPAM have been calculated from the synthesis data shown in Table (1), knowing from these figures that at the low energy region of the absorption edge  $k$  a jump in  $Z_{\text{eff}}$  values will occur due to the occurrence of photoelectric absorption at  $k$  binding energies of the shell. Compounds with high  $Z$  numbers ( $50 < Z$ ) exhibit discontinuities in the  $Z_{\text{eff}}$  spectrum, so this issue does not arise for us because the atomic numbers in our study compounds are ( $Z \leq 20$ ).

The effective atomic number,  $Z_{\text{eff}}$ , was first calculated using the Mayneord formula with the value of  $m=2.94$  [27]:

$$Z_{\text{eff}} = 2.94 \sqrt{\sum_{i=1}^n f_i Z_i^{2.94}} \quad (2)$$

where  $f_i$  is the relative electron fraction of the  $i^{\text{th}}$  element. However, a single value for  $Z_{\text{eff}}$  may be inadequate for mixtures or compounds over a range of energies [28]. The total number of atoms of all types present in the compound. Elemental mass attenuation data over the energy range 1 keV–20 MeV were obtained from the NIST x-ray attenuation database [29]. The cross sections for photoelectric absorption, Compton scattering, and pair production were obtained from the NIST XCOM database [30]. The NIST x-ray attenuation database was also used to obtain elemental data for the mass energy absorption coefficients over the energy range 10 keV–20 MeV, which is a measure of the average reactions occurring within a material within a given unit area of mass [31]. Then, the NIPAM gel and water were calculated using the mixture rule [32]:

$$\left(\frac{\mu}{\rho}\right)_{\text{en}} = \sum_{i=1}^n w_i \left(\frac{\mu}{\rho}\right)_{\text{enj}} \quad (3)$$

Where  $\left(\frac{\mu}{\rho}\right)_{\text{en}}$  is the mass energy absorption coefficient of the compound and  $\left(\frac{\mu}{\rho}\right)_{\text{enj}}$  is the mass energy absorption coefficient of each constituent element in the compound, and  $w_i$  is the fraction by mass of  $i^{\text{th}}$  element. To further investigate the water equivalency of NIPAM dosimetric properties, the



collisional, radiative, and total mass stopping powers for electron beams were also calculated using the NIST ESTAR database over the energy range 10 keV–20 MeV [33]. The GAUSSIAN-09W computer program were used for all calculations and Gauss View 5 molecular visualization programs. One of the oldest and most popular exchange-correlation functionals, the B3LYP hybrid functional, incorporates Lee, Yang, and Parr's correlation functional as well as Becke's three-parameter exchange functional in the DFT calculations

### 3. Results and discussion

#### 3.1 Effective Atomic Number

Within the energy range (10 keV-10MeV),  $Z_{\text{eff}}$  was calculated for water, NIPAM gel, bone, and Tissue, since water is included in all these materials, it is necessary to evaluate the water equivalence, so the ratio of  $Z_{\text{eff}}$  values for each material to  $Z_{\text{eff}}$  values for water within the same energy range was calculated, and this is shown in Figures 2 and 3 to show or interpret these figures, the studied materials have  $Z_{\text{eff}} \approx Z$  and almost have the same composition, we will notice that the figures are roughly similar as the energy changes. Water has  $Z_{\text{eff}}$  as in Figure (1), while other materials showed similarity in the  $Z_{\text{eff}}$  spectrum of water with energy with a small difference that may reach an exponential ratio as in Figures (1) and (2), where the  $Z_{\text{eff}}$  decreases sharply at an energy close to 100 KeV and then remains fairly constant, which is due to the dominance of the Compton effect where the cross section depends linearly on the atomic number  $Z$  at about 1. 25 MeV the probability ratio for a larger pair formation process will appear and  $Z_{\text{eff}}$  will increase .

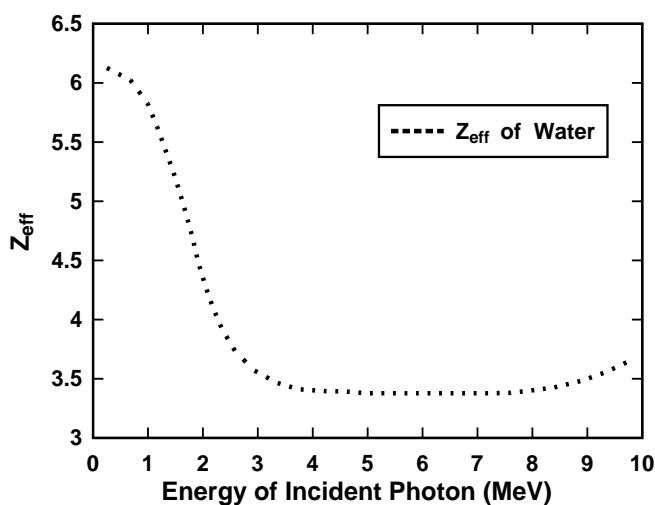


Figure 1: The water effective atomic number for energy range 0.01 keV to 10 MeV



For deviation and depending on the appropriate application for each material and the extent of approximation allowed in the formation of single systems for  $Z_{eff}$  is very appropriate and will therefore take into account the average values of  $Z_{eff}$  within a certain energy range for a radioactive source where three radioactive sources were used to see that their effect on the value of  $Z_{eff}$ , namely  $^{60}\text{Co}$ ,  $^{125}\text{I}$  and  $^{192}\text{Ir}$  for NIPAM, Table (3). The average value for  $Z_{eff}$  was at 106 eV energy for the photon spectrum as measured by Mohanetal This result when compared to the value  $Z_{eff} = 7.37$  according to equation (1) and using  $m=3.5$

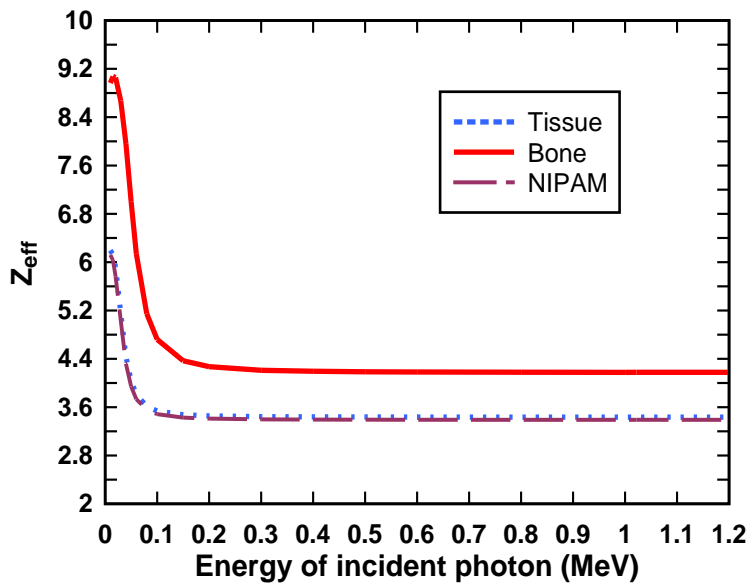


Figure 2: Comparative of  $Z_{eff}$  for each material over energy range.



Table 3: Physical Densities and Zeff for materials, after radiation radioactive sources

Material	Source	$\rho$ (g.cm <sup>3</sup> )	Spectrum weighted of Zeff	Mean Zeff
Water	<sup>60</sup> Co	1.00	3.3349	1.82366
	<sup>125</sup> I		2.26813	2.85255
	<sup>192</sup> Ir		3.29238	3.25494
NIPAN	<sup>60</sup> Co	1.13	3.38997	1.85326
	<sup>125</sup> I		2.27704	2.8594
	<sup>192</sup> Ir		3.345606	3.03668
Bone	<sup>60</sup> Co	1.92	4.17641	2.28688
	<sup>125</sup> I		3.62483	4.49963
	<sup>192</sup> Ir		4.18919	4.30700
Tissue	<sup>60</sup> Co	1.04	3.43471	1.87797
	<sup>125</sup> I		2.31870	2.90992
	<sup>192</sup> Ir		3.39108	3.35385

### 3.2 Gel-Water Equivalence

Here we will use the comparison of mass attenuation coefficients where  $Z_{\text{eff}}$  values depend on them and thus Gel/water equivalence can be discussed. We calculated the result of  $Z_{\text{eff}}(\text{water}) / Z_{\text{eff}}(\text{material})$  and as in Figure (3) where it is clear that the ratios are close to water except for bone as it has  $Z > 20$  and by adopting the change in (test by drawing)  $Z_{\text{eff}}$  which is equivalent to the change in the mass attenuation coefficients for photon energy, we found that NIPAM gel is more compatible with water than tissue, although there is a slight difference in  $Z_{\text{eff}}$  values for both water and NIPAM gel.



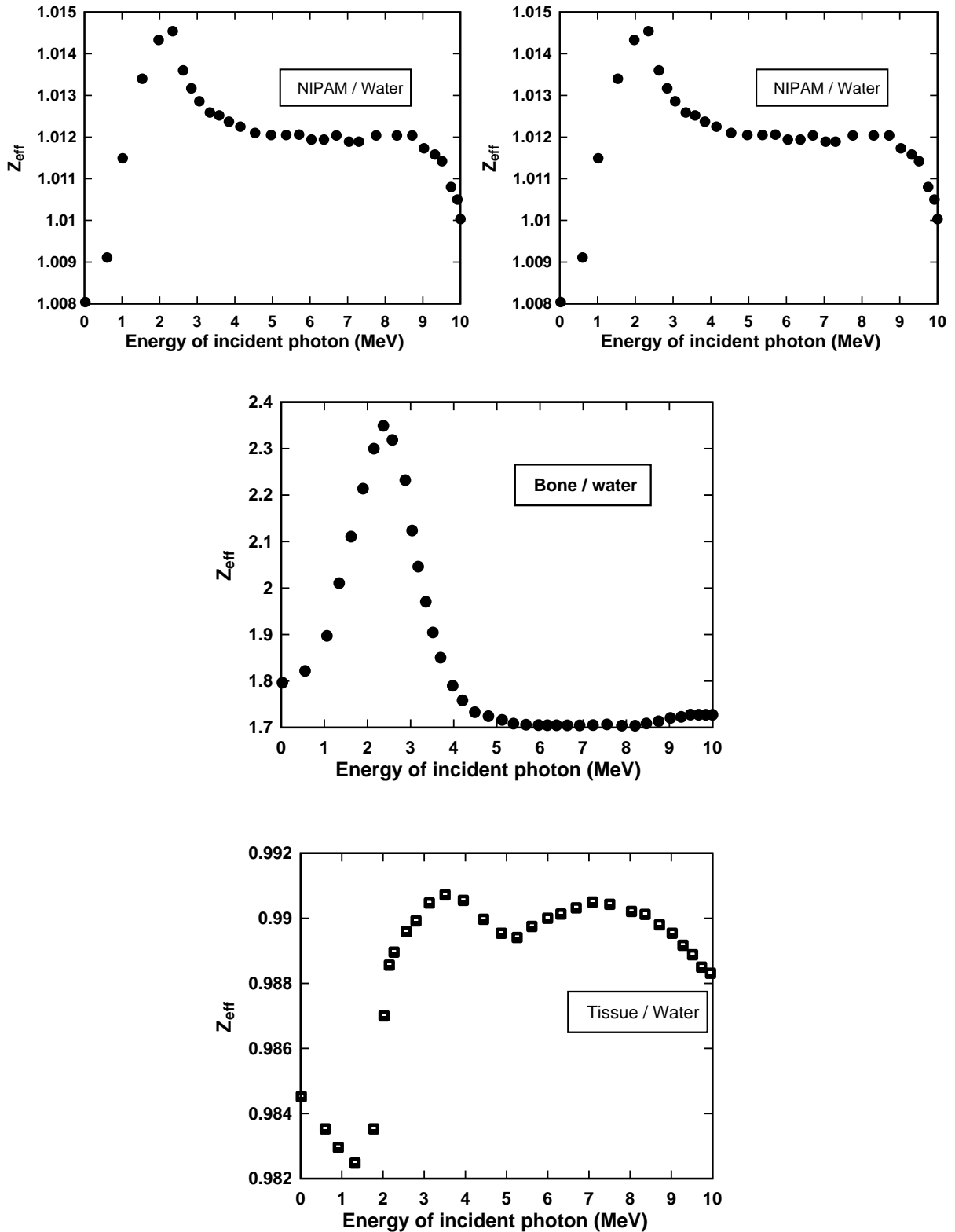


Figure 3: The result of  $Z_{eff}(water) / Z_{eff}(material)$





The variation of the mass attenuation coefficient,  $(\mu/\rho)_{en}$ , Figures (4), calculated at the energy range of incident photon between 0.1 MeV and 100 MeV for four NIPAM gel dosimeters and water. It can be seen from the figure that  $(\mu/\rho)_{en}$  it decreases rapidly as the energy increases from about 0.01 MeV and then starts to slow down. It can be shown in Fig. (4, a) that the rapid decrease at lower energies is due to the photoelectric absorption occurring within the material, where the cross-section of the photon interaction depends on the atomic number of the lower energies. Photon processes in matter are of great importance in medical applications as the cross-sections of these reactions at the energy of the incident photon show us the absorption edge where these cross-sections are interrupted. So, from Fig. (4,b) the sum of the interaction coefficients for the individual processes represents the total attenuation coefficient, and one can see the total interaction cross sections of a photon with NIPAM gel where the Compton scattering is dominant.

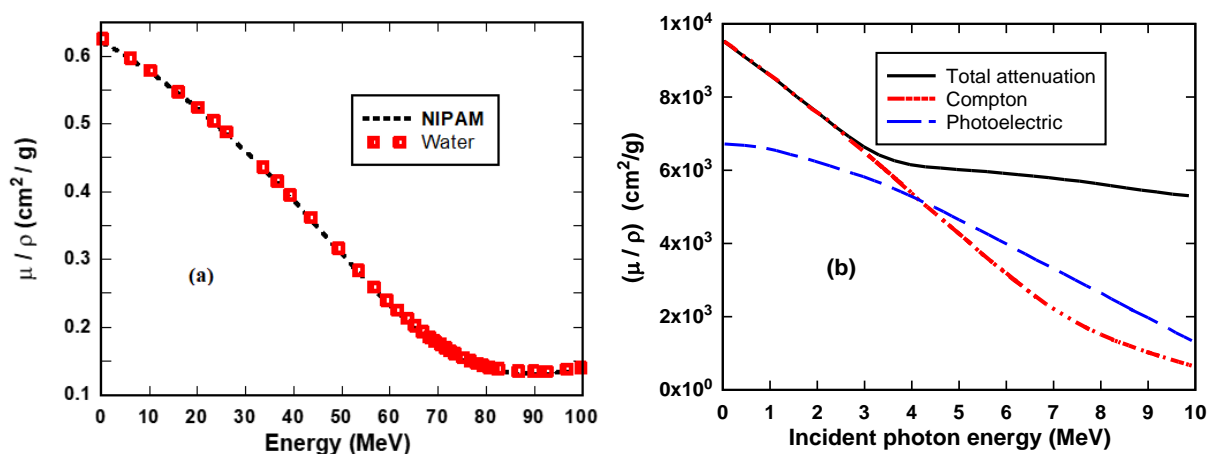


Figure 4: (a) Variations of the mass attenuation coefficient of NIPAM gel dosimeters compares with water as a function of energy. (b) The total cross-section of each photon interaction with matter

Partial reactions with three possibilities are shown in Figure (5) for NIPAM gel synthesis for the energy range of 1 keV to 10 MeV. The figure shows that the photoelectric absorption is negligible at 30 keV due to the dependence of the photoelectric absorption on the atomic number ( $Z^3$ ). As the energy is increased, there is an appearance of the Compton resonance, which is offset by a decrease in the photoelectric interaction due to attenuation. This dominance remains until above 10 MeV, but it starts to decrease gradually at 2-4 MeV due to the attenuation due to the effective atomic number, and at higher energies, the Compton chirality starts to increase and up to 8 MeV the probability of this reaction starts to decrease as it is attributed to the decrease in the



cross-section at higher energies and thus the relative importance of the electron-positron pair production reaction increases, peaking at 10 MeV. This increase in the pair production probability is consistent with the effective atomic number of the gel.

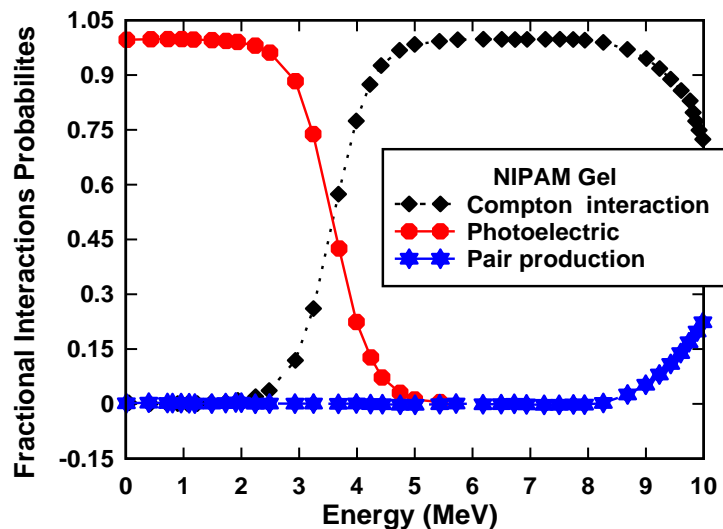


Figure 5: NIPAM dosimeter gel fractional interaction probabilities.

#### 4. Conclusions

In this work, the  $Z_{eff}$  of NIPAM gel was studied as a function of energy for water and compared with three materials: bone, water, and tissue and it was found that the  $Z_{eff}$  of the gel corresponds to water almost better than tissue and bone, taking into account and neglecting the small difference in  $Z_{eff}$  values between NIPAM gel and water and applications that require obtaining a single value of  $Z_{eff}$ , it must be selected according to our calculations that include qualitative or average values of  $Z_{eff}$ . A single  $Z_{eff}$  value should be chosen according to our calculations, which include qualitative or average  $Z_{eff}$  values, and for the purpose of comparison, gel dosimeters or their (radiological) properties should take into account the reaction processes occurring within the water, whether macro or molecular, within the range of energy used.



## References

- [1] A. Lozano, D. Jones, K. Brown, Electron and Positron Scattering Cross Sections from CO<sub>2</sub>: A Comparative Study over a Broad Energy Range (0.1-5000 eV). *J. Phys. Chem. A*, 126(2022) 6032-6046, <https://doi.org/10.1021/acs.jpca.2c05005>
- [2] Z.A. Nezhad, G. Geraily, A review study on application of gel dosimeters in low energy radiation dosimetry. *Appl. Radiat. Isot.*, 179(2022) 110015, <https://doi.org/10.1016/j.apradiso.2021.110015>
- [3] M. Kozicki, J. Nowicki, R. Kalinowski, On the development of a VIPARnd radiotherapy 3D polymer gel dosimeter. *Phys. Med. Biol.*, 62(2017)986, <https://doi.org/10.1088/1361-6560/aa5089>
- [4] A. Venning, B. Hill, C. Baldock, Investigation of the PAGAT polymer gel dosimeter using magnetic resonance imaging. *Phys. Med. Biol.*, 50(2005) 3875, <https://doi.org/10.1088/0031-9155/50/16/015>
- [5] Y. De Deene, N. Reynaert, C. De Wagter, The fundamental radiation properties of normoxic polymer gel dosimeters: a comparison between a methacrylic acid based gel and acrylamide based gels. *Phys. Med. Biol.*, 51(2006) 653, <https://doi.org/10.1088/0031-9155/51/3/012>
- [6] M.Z. Adenan, A. Ahmad, M.F. Khalid, A Study of N-Isopropyl Acrylamide (NIPAM)-Based Polymer Gel Dosimeter by Using Raman Spectroscopy. *Adv. Mater. Res.*, 1107(2015)103-107, <https://doi.org/10.4028/www.scientific.net/AMR.1107.103>
- [7] Y.-J. Chang, X. Li, W. Huang, Quantitative evaluation of an image registration method for a NIPAM gel dosimeter. *Nucl. Instrum. Methods Phys. Res. A*, 784(2015) 542-549, <https://doi.org/10.1016/j.nima.2014.12.075>
- [8] J. Novotny Jr, L. Siskova, J. Novotny, Energy and dose rate dependence of BANG-2 polymer-gel dosimeter. *Med. Phys.*, 28(2001)2379-2386, <https://doi.org/10.1118/1.1414307>
- [9] T. Maeyama, T. Kanai, K. Yusa, Radiological characteristics of MRI-based VIP polymer gel under carbon beam irradiation. *Radiat. Phys. Chem.*, 107(2015) 7-11, <https://doi.org/10.1016/j.radphyschem.2014.09.001>
- [10] P. Kipourous, K. Moutsouris, P. Marinou, Wide dynamic dose range of VIPAR polymer gel dosimetry. *Phys. Med. Biol.*, 46(2001) 2143, <https://doi.org/10.1088/0031-9155/46/8/308>
- [11] Y. Liu, L. Wang, J. Zhang, Environmentally friendly hydrogel: A review of classification, preparation and application in agriculture. *Sci. Total Environ.*, 846(2022)157303, <https://doi.org/10.1016/j.scitotenv.2022.157303>



- [12] Y. De Deene, Radiation dosimetry by use of radiosensitive hydrogels and polymers: mechanisms, state-of-the-art and perspective from 3D to 4D. *Gels*, 8(2022) 599, <https://doi.org/10.3390/gels8090599>
- [13] Y. Huang, A. Stonehouse, C. Abeykoon, Encapsulation methods for phase change materials-A critical review. *Int. J. Heat Mass Transf.*, 200(2023) 123458, <https://doi.org/10.1016/j.ijheatmasstransfer.2022.123458>
- [14] L. Gnanasekaran, V. Kumar, R. Sundararajan, The conversion of biomass to fuels via cutting-edge technologies: Explorations from natural utilization systems. *Fuel*, 331(2023) 125668, <https://doi.org/10.1016/j.fuel.2022.125668>
- [15] J. Cat, N.W. Best, Atomic number and isotopy before nuclear structure: multiple standards and evolving collaboration of chemistry and physics. *Found. Chem.*, 25(2023)67-99, <https://doi.org/10.1007/s10698-022-09450-x>
- [16] E.R. Scerri, Various forms of the periodic table including the left-step table, the regularization of atomic number triads and first-member anomalies. *ChemTexts*, 8(2022) 1-13, <https://doi.org/10.1007/s40828-021-00157-8>
- [17] R.G. Egdell, E. Bruton, Henry Moseley, X-ray spectroscopy and the periodic table. *Philos. Trans. R. Soc. A*, 378(2020) 20190302, <https://doi.org/10.1098/rsta.2019.0302>
- [18] P. Rezaeian, S. Kashian, R. Mehrara, Investigation of the effective atomic number dependency on energy using collision stopping powers for charged particles applied in radiotherapy. *Res. Sq.*, 2168702(2022), v1, <https://doi.org/10.21203/rs.3.rs-2168702/v1>
- [19] M. Hosseini, S. Malekie, M. Keshavarzi, Analysis of Radiation Shielding Characteristics of Magnetite/High Density Polyethylene Nanocomposite at Diagnostic Level Using the MCNPX, XCOM, XMuDat and Auto-Zeff Programs. *Moscow Univ. Phys. Bull.*, 76(2021)S52-S61, <https://doi.org/10.3103/S0027134922010040>
- [20] N.S. Ezra, R. Singh, D. Borjigin, Thermoluminescence properties of Eu<sub>2</sub>O<sub>3</sub>-doped and MgSO<sub>4</sub>-Co-doped Na<sub>2</sub>O silica borate glasses produced by recycling renewable source of soda-lime-silica (SLS). *Opt. Mater.*, 154(2024) 115677, <https://doi.org/10.1016/j.optmat.2024.115677>
- [21] T. Kron, P. Metcalfe, J. Pope, Investigation of the tissue equivalence of gels used for NMR dosimetry. *Phys. Med. Biol.*, 38(1993) 139, <https://doi.org/10.1088/0031-9155/38/1/010>
- [22] L.K. Johnson, J.J. Wirtz, *Intelligence: The Secret World of Spies, an Anthology*. Oxford Univ. Press, (2022).



- [23] H. Tao, Y. Chen, Q. Lin, Textural characteristics of mixed gels improved by structural recombination and the formation of hydrogen bonds between curdlan and carrageenan. *Food Hydrocoll.*, 129(2022)107678, <https://doi.org/10.1016/j.foodhyd.2022.107678>
- [24] R.M. Lokhande, S. Jadhav, S. Pawar, Gamma radiation shielding characteristics of various spinel ferrite nanocrystals: a combined experimental and theoretical investigation. *RSC Adv.*, 11(2021) 7925-7937, <https://doi.org/10.1039/D0RA08372K>
- [25] F.J. Berger, C. Heil, N. Kornienko, How halide alloying influences the optoelectronic quality in tin-halide perovskite solar absorbers. *ACS Energy Lett.*, 8(2023) 3876-3882, <https://doi.org/10.1021/acsenerylett.3c01241>
- [26] L. Guo, H. Zhang, M. Chen, Emerging spintronic materials and functionalities. *Adv. Mater.*, 36(2024) 2301854, <https://doi.org/10.1002/adma.202301854>
- [27] F.M. Khan, *The physics of radiation therapy*. Lippincott Williams & Wilkins, (2010).
- [28] R. Sharma, J. Sharma, T. Singh, Effective atomic numbers for some alloys at 662 keV using gamma rays backscattering technique. *Phys. Sci. Int. J.*, 11(2016)1-6, <https://doi.org/10.9734/PSIJ/2016/27243>
- [29] B. Akça, Ö. Ulusoy, S.Z. Erzenoğlu, Total Mass Attenuation Coefficients, Total Photon Interaction Cross Sections, Effective Atomic Numbers and Effective Electron Densities for Some Construction Materials Available in Turkey. *Arab. J. Sci. Eng.*, 47(2022)7479-7486, <https://doi.org/10.1007/s13369-021-06174-6>
- [30] M. Berger, *XCOM: photon cross sections database*. (2010), <http://www.nist.gov/pml/data/xcom/index.cfm>
- [31] D. Salehi, D. Sardari, M. Jozani, Investigation of some radiation shielding parameters in soft tissue. *J. Radiat. Res. Appl. Sci.*, 8(2015) 439-445, <https://doi.org/10.1016/j.jrras.2015.03.004>
- [32] G.S. Ibbott, Applications of gel dosimetry. *J. Phys. Conf. Ser.*, 3(2004)58-77, <https://doi.org/10.1088/1742-6596/3/1/007>
- [33] C.P. Kumar, T. Srinivasan, M. Chandran, Unified Dosimetry Quality Audit Index: an integrated Monte Carlo model-based quality assurance ranking for radiotherapy treatment of glioblastoma multiforme. *Radiat. Eff. Defects Solids*, 178(2023)258-299, <https://doi.org/10.1080/10420150.2022.2133709>



## الإشعاعية NIPAM دراسة نظرية لخصائص الهلام الإشعاعي لقياس جرعات البوليمر

سويط سمير محمد<sup>1</sup>, اسراء فاخر الشرع<sup>1\*</sup>, اكرم محمد علي<sup>2</sup><sup>1,\*1</sup> قسم الفيزياء, كلية العلوم, الجامعة المستنصرية, بغداد, العراق<sup>2</sup> قسم الفيزياء, كلية العلوم, جامعة الانبار, الانبار, العراق

## المستخلص

في نطاق إجراءات الإشعاع المتقدمة، يقدم NIPAM فرصة هائلة للعمل كقياس جرعات ثلاثي الأبعاد. من أجل استكشاف وتوصيف خصائصه الإشعاعية، استخدمنا مجموعة متنوعة من الطرق المختلفة. مقاطع تفاعل الفوتون، ومعامل امتصاص الطاقة الكتلية، والأعداد الذرية الفعالة، والقيم المتوسطة ل-Zeff، وما يعادل الهلام/الماء. نظرًا للاعتماد الكبير على العدد الذري، فإن مقاطع الامتصاص الضوئي أكبر من مقاطع الماء للطاقات التي تصل إلى 10 ميغا إلكترون فولت. بالمقارنة مع الماء، تتميز المقاطع العرضية لتشتت كومبتون وتوليد الأزواج لهلام NIPAM. نظرًا لحقيقة أن الامتصاص الضوئي هو الوضع السائد لامتصاص الطاقة في نطاق الطاقة هذا، فإن معامل امتصاص الكتلة والطاقة ل-NIPAM أعلى بكثير من معامل الماء. تمت مقارنة النتائج الأولية بنتائج مواد العظام والأنسجة. وقد تم اكتشاف أن Zeff للهلام يرتبط بالماء تقريبًا بالإضافة إلى أي مادة أخرى، بما في ذلك العظام والأنسجة. يمكن إجراء قياس الجرعات باستخدام هلام NIPAM، والذي يمكن اعتباره مكافئًا للماء لكل من keV و MeV، كما هو موضح في نتائجنا. في ضوء هذه النتائج، يمكن الاستنتاج أن هلام NIPAM يتمتع بتكافؤ مائي أعلى مقارنة بالعظام والأنسجة.

